Celestial Mechanics and Dynamical Astronomy (2006) 94:237–248
DOI 10.1007/s10569-005-5533-3

USE OF THE GEOMETRIC ELEMENTS IN NUMERICAL SIMULATIONS

STÉFAN RENNER and BRUNO SICARDY
Observatoire de Paris, LESIA, 92195 Meudon Cédex, France,
e-mail: Stefan.Renner@obspm.fr

(Received: 24 March 2005; revised: 18 October 2005; accepted: 29 November 2005)

Abstract. We derive the transformations to convert the state vector in cartesian coordinates into geometric orbital elements (and conversely the geometric elements into the state vector) for a test particle moving around an oblate planet. These transformations arise from the epicyclic theory and are accurate to second order in eccentricity and inclination. This paper is written to be directly used for computational purposes, such as the numerical study of ring dynamics.

Key words: dynamics, geometric elements, numerical simulations, rings

1. Introduction

The concept of ring streamlines is both powerful and convenient for discussion of a large spectrum of dynamical effects commonly found in ring systems. These streamlines are the lines of the velocity field of the rings considered as a fluid. They are used for example to describe the shape of the narrow rings of Uranus or the density waves of Saturn's rings. For an equatorial ring, the shape of the streamlines is given by:

$$r = a\left[1 - e\cos(m\Phi + m\beta)\right] \tag{1}$$

or by a superposition of sinusoidal terms of the same form, where r is the ring radius, m the azimuthal wave number (integer), β a phase angle, and Φ the longitude in a frame rotating with pattern speed Ω_p, related to the orbital longitude L relative to an inertial reference frame by $\Phi = L - \Omega_p t$. The case of an elliptic ring is included in this description by taking $m = 1$ and $\Omega_p = \dot{\varpi}$, where $\dot{\varpi}$ is the apsidal precession rate.

The orbital elements (semi-major axis a, eccentricity $e, \ldots$) resulting from the fits of Equation (1) to observational data are referred to as the *geometric* elements. They differ from the more familiar *osculating* ones, especially when the planet's oblateness is taken into account. The osculating elements are the elements that particles would have if the oblateness were instantaneously suppressed. When the central body is oblate, the osculating elements exhibit significant short-period variations. The geometric elements also undergo short-period oscillations, but the amplitude is very small and can be neglected.

Furthermore, a particle on a circular orbit around an oblate planet has a non-zero osculating eccentricity $e_0 \sim (3/2) J_2 (R_p/r)^2$. Indeed, the particle's eccentricity would be the osculating eccentricity if the oblateness were suddenly suppressed. The same problem arises with the semimajor axis: the semi-major axis of a particle on a circular orbit around an oblate planet would take the osculating value $a_0 \sim r[1 + (3/2) J_2 (R_p/r)^2]$ if the oblateness were cancelled. For example, $e_0 \sim 0.0045$ and $a_0 \sim 137,650$ km, for a particle on a circular orbit around Saturn with a radius $r = 137,000$ km, corresponding to outer edge of the main rings. Thus the osculating semi-major axis can be substantially different from the geometric radius of the orbit, even if the difference is only relative (whereas it is absolute for the eccentricity). Therefore the geometric elements are the suitable elements to use when considering orbits of satellites (with small eccentricities and inclinations) or ring particles around an oblate planet.

Theoretically, how are they defined these geometric elements? The answer is in the *epicyclic* theory. This theory was initially introduced by Chandrasekar in 1942 in stellar dynamics and deals with the almost circular and almost equatorial motions in an oblate (or prolate) potential. It can be applied to planetary rings because all known rings have small inclinations and small eccentricities. The exact solutions of the equations of motions are series expansion around circular equatorial orbits. The constants arising from these series expansions are the epicyclic elements. The theory also involves three basic frequencies which are the angular velocity of revolution on circular orbits, the horizontal epicyclic frequency κ, which characterizes radial oscillations around the circular motion, and the vertical epicyclic frequency ν, which characterizes vertical oscillations. From the epicyclic elements we can introduce a new set of elements which makes the epicyclic solution analogous to the more familiar elliptic one. These new elements are the geometric elements. The reader will refer to Borderies and Longaretti (1987), Longaretti and Borderies (1991) and Borderies-Rappaport and Longaretti (1994) (hereafter referred to as BL94) for a complete resolution of this problem.

In numerical simulations, the motion of a particle is often integrated in a planet-centered and cartesian reference frame. Then, we must convert the geometric elements into position-velocity vectors (state vector) in a planet-centered cartesian reference frame. This is necessary for instance at the start time of an integration, when only the orbital elements are known at a given epoch. Conversely, we need to convert the state vector of the particle at a given time into geometric elements (as outputs of an integration). The aim of this paper is to give these two sets of transformations (Sections 2 and 3) at a high level of accuracy, and the corresponding numerical implementation. We have applied the results of BL94: the transformations result from the epicyclic theory and are accurate to second order in eccentricity and inclination.

This second order correction can be important in numerical simulations. Let us consider, for instance, the outer shepherd moon for Saturn's F ring, Pandora. Due to a nearby 3:2 co-rotation eccentric resonance with Mimas, Pandora's semi-major axis vary by approximately ± 1.5 km (French et al., 2003). Such an effect cannot be detected in simulations, without taking into account the second-order contributions in eccentricity and inclination. Indeed, if we integrate the motion of Pandora alone (semi-major axis $a \sim 141,700$ km, eccentricity $e \sim 4.5 \times 10^{-3}$) and compute the geometric elements to first order only, then the semi-major axis vary by about ± 10 km.

2. From Geometric Elements to State Vector

Consider a test particle moving around an oblate planet of mass M_p, radius R_p, and zonal harmonic coefficients J_2, J_4 and J_6.

At a given time, the test particle motion is defined by six geometric orbital elements a, e, I, ϖ, Ω, and λ, where a denotes the semi-major axis, e the eccentricity, I the inclination, Ω the longitude of ascending node, ϖ the longitude of periapsis and λ the mean longitude.

The mean longitude has no simple geometrical interpretation: it is defined by $\lambda = M + \varpi = n(t - \tau) + \varpi = (2\pi/T)(t - \tau) + \varpi$, where M, n, τ and T are the mean anomaly, the mean motion, the time of passage at the periapsis and the orbital period of the particle, respectively. The true longitude is defined by $f + \varpi$, where f is the true anomaly.

In the remainder of this paper, r, L, z (resp. x, y, z) is an inertial cylindrical (resp. cartesian) system of coordinates tied to the planet axis and plane of symmetry.

The transformation of the geometric elements into the state vector is straightforward and results from the direct application of the formulae (62–67) of BL94. In cylindrical coordinates, we have:

$$r = a\Big[1 - e\cos(\lambda - \varpi) + e^2\Big(\frac{3}{2}\frac{\eta^2}{\kappa^2} - 1 - \frac{\eta^2}{2\kappa^2}\cos 2(\lambda - \varpi)\Big) + I^2\Big(\frac{3}{4}\frac{\chi^2}{\kappa^2} - 1 + \frac{\chi^2}{4\alpha^2}\cos 2(\lambda - \Omega)\Big)\Big], \tag{2}$$

$$L = \lambda + 2e\frac{n}{\kappa}\sin(\lambda - \varpi) + e^2\Big(\frac{3}{4} + \frac{\eta^2}{2\kappa^2}\Big)\frac{n}{\kappa}\sin 2(\lambda - \varpi) - I^2\frac{\chi^2}{4\alpha^2}\frac{n}{\nu}\sin 2(\lambda - \Omega), \tag{3}$$

$$z = aI\Big[\sin(\lambda - \Omega) + e\frac{\chi^2}{2\kappa\alpha_1}\sin(2\lambda - \varpi - \Omega) - e\frac{3}{2}\frac{\chi^2}{\kappa\alpha_2}\sin(\varpi - \Omega)\Big], \tag{4}$$

$$\dot{r} = a\kappa\Big[e\sin(\lambda - \varpi) + e^2\frac{\eta^2}{\kappa^2}\sin 2(\lambda - \varpi) - I^2\frac{\chi^2}{2\alpha^2}\frac{\nu}{\kappa}\sin 2(\lambda - \Omega)\Big], \tag{5}$$

$$\dot{L} = n\Big[1 + 2e\cos(\lambda - \varpi) + e^2\Big(\frac{7}{2} - 3\frac{\eta^2}{\kappa^2} - \frac{\kappa^2}{2n^2} + \Big(\frac{3}{2} + \frac{\eta^2}{\kappa^2}\Big)\cos 2(\lambda - \varpi)\Big) + I^2\Big(2 - \frac{\kappa^2}{2n^2} - \frac{3}{2}\frac{\chi^2}{\kappa^2} - \frac{\chi^2}{2\alpha^2}\cos 2(\lambda - \Omega)\Big)\Big], \tag{6}$$

$$\dot{z} = aI\nu\Big[\cos(\lambda - \Omega) + e\frac{\chi^2(\kappa + \nu)}{2\kappa\alpha_1\nu}\cos(2\lambda - \varpi - \Omega) + e\frac{3}{2}\frac{\chi^2(\kappa - \nu)}{\kappa\alpha_2\nu}\cos(\varpi - \Omega)\Big]. \tag{7}$$

In cartesian coordinates, we have:

$$x = r\cos L, \tag{8}$$

$$y = r\sin L, \tag{9}$$

$$z = z, \tag{10}$$

$$\dot{x} = \dot{r}\cos L - r\dot{L}\sin L, \tag{11}$$

$$\dot{y} = \dot{r}\sin L + r\dot{L}\cos L, \tag{12}$$

$$\dot{z} = \dot{z}. \tag{13}$$

The formulae (2–7) are accurate to second order in eccentricity and inclination. The terms κ, ν, η, χ, α_1, α_2 and α contain some derivatives of the planetary potential and are homogeneous to frequencies. In particular, κ is the horizontal epicyclic frequency, which characterizes radial oscillations around the circular motion ($\kappa = n - \dot{\varpi}$ where $\dot{\varpi}$ is the apsidal precession rate of the test particle), and ν is the vertical epicyclic frequency, which characterizes vertical oscillations ($\nu = n - \dot{\Omega}$ where $\dot{\Omega}$ is the precession rate of the ascending node). To second order in eccentricity and inclination, the frequencies are given by:

$$n = \sqrt{\frac{GM_p}{a^3}}\Big[1 + \frac{3}{4}\Big(\frac{R_p}{a}\Big)^2 J_2 - \frac{15}{16}\Big(\frac{R_p}{a}\Big)^4 J_4 + \frac{35}{32}\Big(\frac{R_p}{a}\Big)^6 J_6 - \frac{9}{32}\Big(\frac{R_p}{a}\Big)^4 J_2^2 + \frac{45}{64}\Big(\frac{R_p}{a}\Big)^6 J_2 J_4 + \frac{27}{128}\Big(\frac{R_p}{a}\Big)^6 J_2^3 + 3\Big(\frac{R_p}{a}\Big)^2 J_2 e^2 - 12\Big(\frac{R_p}{a}\Big)^2 J_2 I^2\Big], \tag{14}$$

$$\kappa = \sqrt{\frac{GM_p}{a^3}}\Big[1 - \frac{3}{4}\Big(\frac{R_p}{a}\Big)^2 J_2 + \frac{45}{16}\Big(\frac{R_p}{a}\Big)^4 J_4 - \frac{175}{32}\Big(\frac{R_p}{a}\Big)^6 J_6 - \frac{9}{32}\Big(\frac{R_p}{a}\Big)^4 J_2^2 + \frac{135}{64}\Big(\frac{R_p}{a}\Big)^6 J_2 J_4 - \frac{27}{128}\Big(\frac{R_p}{a}\Big)^6 J_2^3 - 9\Big(\frac{R_p}{a}\Big)^2 J_2 I^2\Big], \tag{15}$$

$$\nu = \sqrt{\frac{GM_p}{a^3}}\Big[1 + \frac{9}{4}\Big(\frac{R_p}{a}\Big)^2 J_2 - \frac{75}{16}\Big(\frac{R_p}{a}\Big)^4 J_4 + \frac{245}{32}\Big(\frac{R_p}{a}\Big)^6 J_6 - \frac{81}{32}\Big(\frac{R_p}{a}\Big)^4 J_2^2 + \frac{675}{64}\Big(\frac{R_p}{a}\Big)^6 J_2 J_4 + \frac{729}{128}\Big(\frac{R_p}{a}\Big)^6 J_2^3 + 6\Big(\frac{R_p}{a}\Big)^2 J_2 e^2 - \frac{51}{4}\Big(\frac{R_p}{a}\Big)^2 J_2 I^2\Big], \tag{16}$$

$$\eta^2 = \frac{GM_p}{a^3}\Big[1 - 2\Big(\frac{R_p}{a}\Big)^2 J_2 + \frac{75}{8}\Big(\frac{R_p}{a}\Big)^4 J_4 - \frac{175}{8}\Big(\frac{R_p}{a}\Big)^6 J_6\Big], \tag{17}$$

$$\chi^2 = \frac{GM_p}{a^3}\Big[1 + \frac{15}{2}\Big(\frac{R_p}{a}\Big)^2 J_2 - \frac{175}{8}\Big(\frac{R_p}{a}\Big)^4 J_4 + \frac{735}{16}\Big(\frac{R_p}{a}\Big)^6 J_6\Big], \tag{18}$$

$$\alpha_1 = \frac{1}{3}(2\nu + \kappa), \tag{19}$$

$$\alpha_2 = 2\nu - \kappa, \tag{20}$$

$$\alpha^2 = \alpha_1 \alpha_2. \tag{21}$$

All these frequencies reduce to the Keplerian mean motion $\sqrt{GM_p/a^3}$ if the planet is spherical. The relations (14), (15), ... , (21) correspond respectively to (A10), (A12), (A11), (A4), (A5), (36), (37) and (38) of BL94.

Remark. There are misprints in the original paper (BL94): the last term (proportional to I^2) in the right-hand side member of Equation (65) should have a minus instead of a plus. In Equation (6), the second and third terms in the right-hand side member should have a ν_a in the denominator instead of a ν_0. Here we have applied these corrections (where $\nu \equiv \nu_a$), see Equations (5) and (7).

3. From State Vector to Geometric Elements

Let $\mathbf{v} = (x, y, z, \dot{x}, \dot{y}, \dot{z})$ be the state vector of the test particle in the planet-centered cartesian reference frame $(O\mathbf{xyz})$. In cylindrical coordinates, $\mathbf{v} = (r, L, z, \dot{r}, \dot{L}, \dot{z})$, where:

$$r = \sqrt{x^2 + y^2}, \tag{22}$$

$$L = \arctan(y/x), \tag{23}$$

$$\dot{r} = \dot{x}\cos L + \dot{y}\sin L, \tag{24}$$

$$\dot{L} = (-\dot{x}\sin L + \dot{y}\cos L)/r. \tag{25}$$

Note that the longitude L is defined on $[0, 2\pi]$ whereas $\arctan(\mathbb{R}) =]-\pi/2, \pi/2[$. Therefore, it must be modified in the following cases:

$$L = \arctan(y/x) + \pi \qquad x < 0, \tag{26}$$

$$L = \arctan(y/x) + 2\pi \qquad \arctan(y/x) < 0, \tag{27}$$

$$L = \pi/2 \qquad x = 0 \;\; y > 0, \tag{28}$$

$$L = 3\pi/2 \qquad x = 0 \;\; y < 0. \tag{29}$$

The transformations (2–7) can be written:

$$r = a\Big[1 - e\cos(\lambda - \varpi)\Big] + r_C, \tag{30}$$

$$L = \lambda + 2e\frac{n}{\kappa}\sin(\lambda - \varpi) + L_C, \tag{31}$$

$$z = aI\sin(\lambda - \Omega) + z_C, \tag{32}$$

$$\dot r = ae\kappa\sin(\lambda - \varpi) + \dot r_C, \tag{33}$$

$$\dot L = n\Big[1 + 2e\cos(\lambda - \varpi)\Big] + \dot L_C, \tag{34}$$

$$\dot z = aI\nu\cos(\lambda - \Omega) + \dot z_C, \tag{35}$$

where r_C, L_C, z_C, $\dot r_C$, $\dot L_C$ and $\dot z_C$ contain all the terms of second order in eccentricity and inclination. More precisely:

$$\begin{aligned} r_C = {} & ae^2\left[\frac{3}{2}\frac{\eta^2}{\kappa^2} - 1 - \frac{\eta^2}{2\kappa^2}\cos 2(\lambda - \varpi)\right] \\ & + aI^2\left[\frac{3}{4}\frac{\chi^2}{\kappa^2} - 1 + \frac{\chi^2}{4\alpha^2}\cos 2(\lambda - \Omega)\right], \end{aligned} \tag{36}$$

$$L_C = e^2\left(\frac{3}{4} + \frac{\eta^2}{2\kappa^2}\right)\frac{n}{\kappa}\sin 2(\lambda - \varpi) - I^2\frac{\chi^2}{4\alpha^2}\frac{n}{\nu}\sin 2(\lambda - \Omega), \tag{37}$$

$$z_C = aIe\left[\frac{\chi^2}{2\kappa\alpha_1}\sin(2\lambda - \varpi - \Omega) - \frac{3}{2}\frac{\chi^2}{\kappa\alpha_2}\sin(\varpi - \Omega)\right], \tag{38}$$

$$\dot r_C = ae^2\frac{\eta^2}{\kappa}\sin 2(\lambda - \varpi) - aI^2\frac{\chi^2}{2\alpha^2}\nu\sin 2(\lambda - \Omega), \tag{39}$$

$$\begin{aligned} \dot L_C = {} & e^2 n\left[\frac{7}{2} - 3\frac{\eta^2}{\kappa^2} - \frac{\kappa^2}{2n^2} + \left(\frac{3}{2} + \frac{\eta^2}{\kappa^2}\right)\cos 2(\lambda - \varpi)\right] \\ & + I^2 n\left[2 - \frac{\kappa^2}{2n^2} - \frac{3}{2}\frac{\chi^2}{\kappa^2} - \frac{\chi^2}{2\alpha^2}\cos 2(\lambda - \Omega)\right], \end{aligned} \tag{40}$$

$$\dot z_C = aIe\Big[\frac{\chi^2(\kappa + \nu)}{2\kappa\alpha_1}\cos(2\lambda - \varpi - \Omega) + \frac{3}{2}\frac{\chi^2(\kappa - \nu)}{\kappa\alpha_2}\cos(\varpi - \Omega)\Big]. \tag{41}$$

We must derive the geometric orbital elements, knowing the position and the velocity of the test particle, i.e. r, L, z, $\dot{r}$, $\dot{L}$, $\dot{z}$. From (30–35) we have:

$$a = \frac{r - r_C}{1 - \dfrac{\dot{L} - \dot{L}_C - n}{2n}}, \tag{42}$$

$$e = \sqrt{\left(\frac{\dot{L} - \dot{L}_C - n}{2n}\right)^2 + \left(\frac{\dot{r} - \dot{r}_C}{a\kappa}\right)^2}, \tag{43}$$

$$I = \sqrt{\left(\frac{z - z_C}{a}\right)^2 + \left(\frac{\dot{z} - \dot{z}_C}{a\nu}\right)^2}, \tag{44}$$

$$\lambda = L - L_C - 2\frac{n}{\kappa}\frac{\dot{r} - \dot{r}_C}{a\kappa}, \tag{45}$$

$$\tan(\lambda - \varpi) = \frac{\dot{r} - \dot{r}_C}{a\kappa\left(1 - \dfrac{r - r_C}{a}\right)}, \tag{46}$$

$$\tan(\lambda - \Omega) = \nu\frac{z - z_C}{\dot{z} - \dot{z}_C}. \tag{47}$$

We compute a, e, I, λ, ϖ and Ω from the relations (42–47) by an iterative method on the frequencies n, κ, ν, η and χ:

– first, we assume that $a = r$, $e = I = 0$ and that $r_C = L_C = z_C = \dot{r}_C = \dot{L}_C = \dot{z}_C = 0$.
– We compute all the frequency values from (14–21), which yield new values for the geometric elements (42–47) and for r_C, L_C, z_C, $\dot{r}_C$, $\dot{L}_C$, $\dot{z}_C$ (36–41).
  Note that ϖ and Ω must be modified in some cases, as in (26–29) for the longitude L, since they are computed from the arctan function (46–47).
– Then we compute again the frequencies (14–24), the geometric elements (42–47), the second order terms (36–41), and so on until the iteration converges (this convergence is very fast).
– To stop the iteration and store the orbital elements, we introduce the following simple test on the semi-major axis: $|a_{i+1} - a_i| < \epsilon$, where ϵ is a prescribed small strictly positive parameter, and a_i is the ith value of the semi-major axis computed in the iteration.

As required, the orbital elements derived are accurate to second order in eccentricity and inclination. However, we can use an integral of the motion (the vertical component of the angular momentum) to compute a more accurate value for the semi-major axis.

Let H_z be the vertical angular momentum of the test particle, and r_0 the radius of the equatorial circular orbit around which the solution r, L, z is expanded. We can always choose the radius r_0 such that the vertical angular momentum of the solution H_z is equal to the angular momentum of the equatorial circular orbit, i.e.:

$$H_z \equiv x\dot{y} - y\dot{x} = r_0^2 n_0, \tag{48}$$

where, considering terms up to and including J_6, the mean motion n_0 above is defined by:

$$n_0^2 = \frac{GM_p}{r_0^3}\left[1 + \frac{3}{2}\left(\frac{R_p}{r_0}\right)^2 J_2 - \frac{15}{8}\left(\frac{R_p}{r_0}\right)^4 J_4 + \frac{35}{16}\left(\frac{R_p}{r_0}\right)^6 J_6\right]. \tag{49}$$

The formula (49) is the relation (A3) of BL94. As explained in BL94 (see Equation 56), the geometric elements a, e, I and the radius r_0 are related by:

$$a = r_0(1 + e^2 + I^2) \tag{50}$$

Therefore, for a given state vector of the test particle, we compute iteratively the value of r_0 using (48–49), and we deduce the semi-major axis a from (50), using the values of e and I determined with the previous iteration (42–47).

Remark. Let us suppose that we want to integrate numerically the motion of a test particle with given orbital elements a_p, e_p, I_p, following the numerical implementation proposed in this paper. Then, we must choose at the start of the simulation a different initial semi-major axis $a_p \pm c_3$, where c_3 is a third order correction term in eccentricity and inclination. Indeed, the semi-major axis value, $r_0(1 + e_p^2 + I_p^2)$, computed during the integration from the vertical angular momentum H_z (48–50), is initially different from a_p: the difference is of order three, since the transformations (2–7) that convert initially the geometric elements into the state vector are accurate to second order in eccentricity and inclination. The exact c_3 value is determined numerically (see Section 4) and depends on the initial phases.

4. Application

The orbital elements derived with our method are accurate for the description of the orbits of most of the planetary satellites and ring particles, with typical eccentricities $e \sim 0.001, 0.01$ and inclinations $I \sim 1^\circ$ or less.

Here we consider a typical example. We use the *mercury* 6 integrator package (Chambers, 1999), with a Bulirsch-Stoer algorithm, and an accuracy parameter $\delta = 10^{-12}$, the relative error per step the algorithm tolerates. The motion is integrated in cartesian coordinates in a reference frame centered on the central body.

We consider a test particle on an eccentric and inclined orbit around Saturn, with $a = 150, 000$ km, $e = 0.01$ and $I = 0.5^\circ$. The physical parameters of Saturn (mass, radius and oblateness) are given in Table I (Campbell and Anderson, 1989).

We assume that, initially, $\varpi = \Omega = 90^\circ$ and $\lambda = 0$. The integration time is equal to the orbital period $T_{\rm ORB} = 0.6846$ days of the test particle. The particle is launched with the following initial value for the semi-major axis: $150, 000.497$ km. Thus, the mean value over one orbital period $T_{\rm ORB}$ for the semi-major axis a, as derived from Equations (48–50), is equal to the prescribed value of 150,000 km (see the Remark at the end of Section 3).

The variations of the orbital elements a, e, I, as calculated from Equations (48–50), (43) and (44), respectively, are presented in Figure 1. The amplitudes of these variations are independent from the initial phases, and are of order three in eccentricity and inclination. In particular, the maximum variation for the semi-major axis, as defined in Equation (50), is here $\Delta a \sim 40$ m (Figure 1). If we derive a from the iteration (42–47), then we obtain a maximum variation $\Delta a \sim 1.5$ km. This shows why we deduce the semi-major axis from the vertical angular momentum, see Equations (48–50). Furthermore, let us remark that if we do not take into account the second order contributions in e and I, then $\Delta a \sim 100$ km for the same orbit.

Short-period variations of the longitude of periapsis, the longitude of ascending node or the mean longitude are extremely small and are not presented here.

TABLE I

Saturn's physical parameters, from Campbell and Anderson (1989).

GM_p (km^3 s^{-2})	R_p (km)	J_2	J_4	J_6
3.7931272×10^7	60330.	16298×10^{-6}	-915×10^{-6}	103×10^{-6}

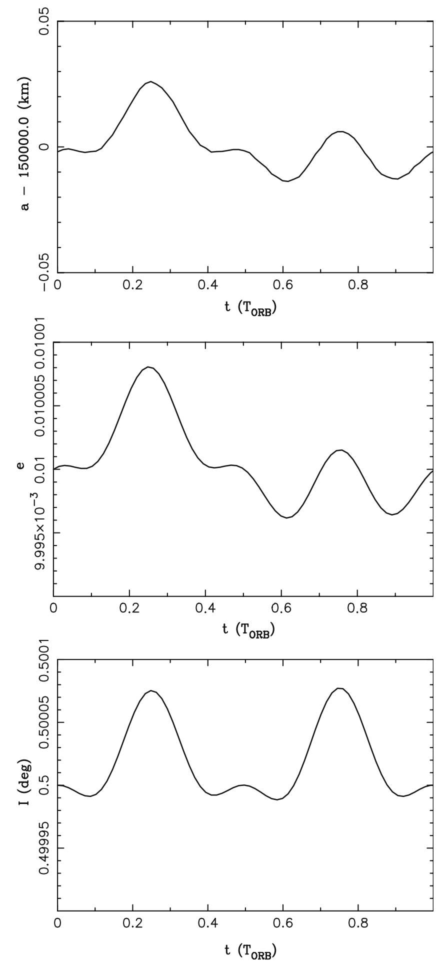

Figure 1. Geometric semi-major axis a, eccentricity e and inclination I versus time (in units of the orbital period T_{ORB} of the test particle). The other initial conditions are $\varpi = \Omega = 90^\circ$ and $\lambda = 0$. The maximum variations for a, e and I are respectively $\Delta a = 3.9 \times 10^{-2}$ km, $\Delta e = 1.2 \times 10^{-5}$ and $\Delta I = 1.6 \times 10^{-6}$ rad. For comparison, if we compute the geometric elements to first order in e and I only, the maximum variations for a, e and I are respectively: $\Delta a = 99.001$ km, $\Delta e = 8.7 \times 10^{-4}$ and $\Delta I = 1.8 \times 10^{-4}$ rad.

Acknowledgements

We are grateful to Pierre-Yves Longaretti for constructive suggestions.

References

Borderies, N. and Longaretti, P.-Y.: 1987, 'Description and behavior of streamlines in planetary rings', *Icarus* **72**, 593–603.

Borderies-Rappaport, N. and Longaretti, P.-Y.: 1994, 'Test particle motion around an oblate planet', *Icarus* **107**, 129–141.

Campbell, J. K. and Anderson, J. D.: 1989, 'Gravity field of the saturnian system from *Pioneer* and *Voyager* tracking data', *AJ* **97**, 1485–1495.

Chambers, J. E.: 1999, 'A hybrid symplectic integrator that permits close encounters between massive bodies', *MNRAS* **304**, 793–799.

French, R. G., McGhee, C. A., Dones, L. and Lissauer, J. J.: 2003, 'Saturn's wayward shepherds: the peregrinations of Prometheus and Pandora', *Icarus*, **162**, 143–170.

Longaretti, P.-Y. and Borderies, N.: 1991, 'Streamline formalism and ring orbit determination', *Icarus* **94**, 165–170.